IEEE Transactions on Aerospace and Electronic Systems,
Volume 58, Number 4, August 2022, pp. 3708-3716
DOI: 10.1109/TAES.2022.3153758

$\mathcal{L}_1$ Adaptive Path-Following of Small Fixed-wing Unmanned Aerial Vehicles in Wind

Toufik Souanef

Abstract

This paper proposes an adaptive path-following controller of small fixed-wing Unmanned Aerial Vehicles (UAVs) in the presence of wind disturbances, which explicitly considers that wind speed is time-varying. The main idea was to formulate UAVs path-following as control design for systems with parametric uncertainties and external disturbances. Assuming that there is no prior information on wind, the proposed solution is based on the $\mathcal{L}_1$ adaptive control, using linearized model dynamics. This approach makes clear statements for performance specifications of the controller and relaxes the common constant wind velocity assumption. This makes the design more realistic and the analysis more rigorous, because in practice wind is usually time varying (windshear, turbulence and gusting). The path-following controller was demonstrated in flight under wind speed up to 10m/s, representing 50% of the nominal UAV airspeed.

Index Terms

UAV Path-Following; UAV Control; $\mathcal{L}_1$ Adaptive Control

I. Introduction

Small fixed-wing UAVs (that is, with wingspans less than 2 metres and payload smaller than 2 kg) have gained growing interest because of their low cost, high maneuverability and simple maintenance. They are used for a wide range of military and civilian tasks [1]. Many UAVs applications require the system to autonomously follow a desired path [2]. The objective of the path-following system is to generate commands to the attitude controller in order to follow a given reference trajectory. Path-following of fixed-wing UAVs is usually designed based on missile guidance [3] and control techniques, particularly nonlinear control [4]. A survey of different path-following approaches for fixed-wing UAVs is given in [2].

T. Souanef is with Cranfield University, Cranfield, United Kingdom (e-mail: toufik.souanef@cranfield.ac.uk).

However, small UAVs path-following is still a challenging problem because of their extreme sensitivity to wind because of their relatively low speeds. For such UAVs, wind speeds are commonly 20% to 60% of the desired airspeed [5]. If the path-following (guidance) system does not account for wind, the trajectory tracking ability of UAVs will be reduced. Therefore, there is a need to design path-following methods that are explicitly robust against wind disturbances.

The previous approaches dealing with fixed-wing UAVs path-following in wind are based on the modification of the planned path [6]–[9] and control [5], [10]–[15]. Their common issue is that they assume that wind speed is constant. In [16] an adaptive control design for UAV path-following with slowly time-varying wind is presented. All these assumptions are not realistic, because wind velocity is not constant in practice, and it can change quickly. More recently, a path-following algorithm for fixed-wing UAVs by virtue of a nonlinear optimal control approach and wind disturbance sliding mode observers was developed in [17]. The design of the controller assumes that there are no parametric uncertainties in the model. This is not the case in practice, as it is not possible to maintain a constant airspeed in real flight conditions, especially in the presence of wind. Furthermore, a disadvantage of sliding mode observers is that they may not respond rapidly and if wind speed/direction changes quickly, the observer cannot track it easily which may produce the chattering phenomenon.

A solution to this challenge can be provided through the use of $\mathcal{L}_1$ adaptive control [18]. The benefit of $\mathcal{L}_1$ adaptive control is its capacity for fast and robust adaptation that leads to desired transient performance for both system signals, input and output. These characteristics make it suitable for systems subject to external time-varying disturbances, such as small UAVs motion in wind. The $\mathcal{L}_1$ adaptive control has been applied for various autonomous flight control systems including fixed-wing UAVs [19]–[23] and rotorcraft UAVs [24]–[27], to cite a few.

The main idea of this work, based on [28], is to formulate the path-following of fixed-wing UAVs as control design for systems in the presence of parametric uncertainties and external disturbances. Assuming that there is no prior information on wind, the proposed solution is based on the $\mathcal{L}_1$ adaptive controller for disturbances of unknown bounds [29]. This approach relaxes what is commonly assumed that wind speed is constant.

It should be noted that $\mathcal{L}_1$ adaptive control has not been used previously for the design of fixed-wing UAVs guidance system. In [2] it is stated that $\mathcal{L}_1$ adaptive control is applied in [21], [30] to the path-following of a fixed-wing UAV, while in fact, the $\mathcal{L}_1$ adaptive controller augments the low-level controller in the presence of uncertainties and external disturbances. In

[31]–[33] the $\mathcal{L}_1$ adaptive controller is applied to attitude control of quadrotors, hypersonic reentry vehicles and ships, respectively, but not to the path-following system. An $\mathcal{L}_1$ adaptive trajectory tracking controller for multirotor UAVs in the presence of modelling uncertainties and external disturbances was proposed in [34]. However, the problem of path-following and trajectory tracking for multirotors has a fundamental difference to that of fixed-wing UAVs. The formulation of fixed-wing UAVs path-following is based on the airspeed [2], while for multirotor it is based on the inertial speed [35] that ignores implicitly wind speed effect on the system kinematics. The main motivation of [34] has been to design a robust trajectory tracking controller against unmodeled dynamics that may be present in the inner-loop controlled plant that is also based on the same $\mathcal{L}_1$ adaptive controller, which might be a contradiction.

The contributions of this paper are:

- Formulating the path-following problem as control design in the presence of unknown uncertainties and external disturbances.
- Developing an adaptive path-following controller that is explicitly robust against time-varying wind.
- Demonstrating the performance of the proposed design in simulations as well as in real flight experiments.

To this end, Section 2 develops the path-following problem. Section 3 introduces $\mathcal{L}_1$ adaptive straight-line path-following in the horizontal plane. Section 4 summarises the main results of $\mathcal{L}_1$ adaptive control of systems with disturbances of unknown bounds. Finally, Sections 5 and 6 analyse simulation and flight test results, respectively.

II. The Path-Following Problem

In practice, the two most commonly used paths for UAVs are straight-lines and circular paths [2]. Both types of paths are usually defined on the horizontal plane, with constant altitude and speed. Under these assumptions, the UAV kinematics can be written as follows

$$\begin{aligned} \dot{p}_n &= V_a \cos(\psi) + W_n, \\ \dot{p}_e &= V_a \sin(\psi) + W_e, \end{aligned} \tag{1}$$

where p_n, p_e are respectively the North and East positions, V_a is the airspeed, ψ is the heading angle relative to the north, and W_n and W_e are wind speeds in the inertial frame.

This model is derived under the assumption that the UAV is in steady level flight. In this case, the airspeed vector is aligned with the x-direction of the body frame, which means that the sideslip angle β is zero.

Assuming a coordinated turn, i.e., the ailerons are used to change the UAV heading, the rate of variation of the heading angle is given by

$$\dot{\psi} = \frac{g}{V_a} \tan(\phi). \tag{2}$$

The objective is to compute the desired rolling angle ϕ_c that maintains the UAV on the desired path, despite the presence of wind.

Assumption 1. There is no available information on the wind velocity, given that wind disturbances vary and are often not easily predicted.

Remark 1. In this paper the time dependence of the variables is dropped unless if it is not clear from the context.

III. $\mathcal{L}_1$ Adaptive Straight-Line Path-Following in the Horizontal Plane

The desired path is defined by a straight-line from the precedent waypoint $P_k(p_{nk}, p_{ek})$ to the destination waypoint $P_{k+1}(p_{nk+1}, p_{ek+1})$, where (p_{nk}, p_{ek}) and (p_{nk+1}, p_{ek+1}) are respectively the horizontal coordinates of the waypoints P_k and P_{k+1} in the inertial frame, as shown in Fig. 1.

The cross-track error d is the shortest distance from the position of the UAV to the reference path, given by

$$d = -(p_n - p_{nk}) \sin(\psi_p) + (p_e - p_{ek}) \cos(\psi_p), \tag{3}$$

where ψ_p is the orientation of the path relative to the North direction defined by

$$\psi_p = \text{atan2}(p_{ek+1} - p_{ek}, p_{nk+1} - p_{nk}). \tag{4}$$

By differentiating (3) with respect to time and using (1) and (2), it follows that

$$\begin{aligned} \dot{d} &= -V_a \sin(\psi_e) + W_e \sin(\psi_p) - W_n \cos(\psi_p), \\ \dot{\psi}_e &= -\frac{g}{V_a} \tan(\phi_c), \end{aligned} \tag{5}$$

where $\psi_e = \psi_p - \psi$ is the orientation of the UAV relative to the desired path.

Remark 2. The use of the notations ϕ_c is justified by the fact that, in practice, this angle is the reference input of the low-level controller.

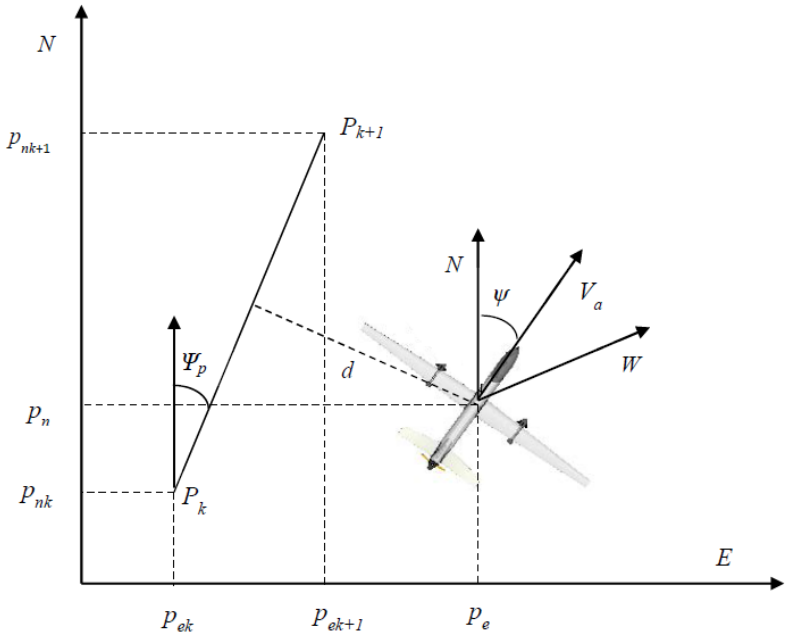

Fig. 1: Path-following in the horizontal plane.

Letting $x = [d, \quad \psi_e]^\top$ be the state vector and $u = \phi_c$ be the control input, the system is transformed to the following nonlinear state-space model

$$\dot{x} = f(x, u) + \zeta, \tag{6}$$

where $f(x,u) = \begin{bmatrix} -V_a \sin(x_2) \\ -\frac{g}{V_a}\tan(u) \end{bmatrix}$ and $\zeta(t) = \begin{bmatrix} W_e \sin(\psi_p) - W_n \cos(\psi_p) \\ 0 \end{bmatrix}$.

The regulated output y is the cross-track error d, i.e., the output vector is

$$c = [1 \quad 0]^\top.$$

The objective is to design the control law $u(t)$ that stabilizes the system and consequently steers the UAV to the reference path. The proposed solution is based on the $\mathcal{L}_1$ adaptive controller. To this end, the linearized model is first derived. Actually, a common procedure in adaptive control design is to linearize the nonlinear model at a given equilibrium or operating point, to design a linear controller based on the linearized system model, and to augment the linear controller with the adaptive controller. This allows for better robustness of the adaptive control system [36].

For the equilibrium point $x_{eq} = [d_{eq} \quad 0]^\top$, $u_{eq} = 0$ and $\zeta_{eq} = 0$, where d_{eq} is arbitrary, the linearized state space model of (6) is given by

$$\dot{\bar{x}} = A_p \bar{x} + b_p \bar{u}, \tag{7}$$

where

$$A_p = \begin{bmatrix} 0 & -V_a \\ 0 & 0 \end{bmatrix}, \quad b_p = \begin{bmatrix} 0 \\ -\frac{g}{V_a} \end{bmatrix}.$$

The obtained model is a standard double integrator system representing single-degree-of-freedom translational and rotational motion. Control of the double integrator has been of interest since the early days of control theory when it was used extensively to illustrate minimum-time and minimum-fuel controllers [37].

Hence, the non-linear system in (6) can be written as follows

$$\dot{x} = A_p x + b_p u + \tilde{f}, \tag{8}$$

where $\tilde{f}(x, u, t)$ is a nonlinear function that includes the higher order terms of the Taylor series expansion of $f(x, u)$ and the external disturbance $\zeta(t)$.

It is important to underline that the matrix A_p and the vector b_p are uncertain because it not possible in real flight conditions to maintain a constant airspeed V_a, especially in the presence of wind.

Moreover, taking into account the dynamics of the attitude controller we have

$$\phi = F(s)\phi_c, \tag{9}$$

where $F(s)$ in an unknown Laplace transfer function.

Therefore, the system in (8) can be written as

$$\dot{x} = A_m x + b\,\omega\,u + (A_p - A_m)x + \tilde{f}, \tag{10}$$

where $A_m = A - b\,k_p^\top$ is a Hurwitz matrix of the desired dynamics of the system, b is the input vector of the system with the nominal airspeed, $k_p \in \mathbb{R}^2$ is the feedback vector, and $\omega \in \mathbb{R}$ is an unknown gain that includes the dynamics of the attitude controller and the airspeed uncertainty.

For control design, the following approximation can be used

$$(A_p - A_m)x + \tilde{f} = b\big(\theta^\top x + \eta_m\big) + \eta_u, \tag{11}$$

where $\theta \in \mathbb{R}^2$ is a vector of unknown parameters, $\eta_m(t) \in \mathbb{R}$ is a matched disturbance and $\eta_u(t,x) \in \mathbb{R}^2$ is a vector of unmatched disturbances.

Consequently, the system in (10) leads to

$$\dot{x} = A_m x + b\big(\omega\, u + \theta^\top x + \eta_m\big) + \eta_u. \tag{12}$$

The resulting model makes straightforward the application of the $\mathcal{L}_1$ adaptive controller that is described later. The block diagram of fixed-wing UAV path-following in wind, based on $\mathcal{L}_1$ adaptive control, is illustrated in Fig. 2.

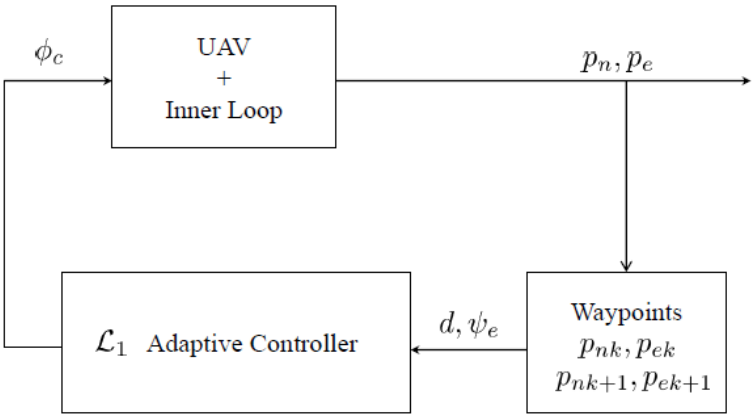

Fig. 2: $\mathcal{L}_1$ adaptive path-following.

Remark 3. The main advantage of the application of $\mathcal{L}_1$ adaptive control to UAV path-following in wind is that good performance of the system can be obtained, whether the unknown wind velocity is constant or not. This is a direct consequence of what was demonstrated in [29] that the $\mathcal{L}_1$ adaptive controller presents a good compromise between performance and robustness in the presence of disturbances with unknown bounds.

Remark 4. Due to lack of space, circular path-following is omitted here. The used approach is similar to straight-line paths. The interested reader is referred to [28].

Remark 5. The altitude hold controller can be designed based on the following

$$\dot{h} = V_a \sin(\gamma_a) - W_d, \tag{13}$$

where h is the altitude of the UAV in the inertial frame, γ_a is the air referenced flight path angle, and W_d is wind speed in the inertial frame.

Hence

$$\dot{h}_e = -V_a \sin(\gamma_a) + W_d, \tag{14}$$

where $h_e = h_d - h$ and h_d the desired altitude.

This formulation is the first order case of the model in (5). The $\mathcal{L}_1$ adaptive controller is straightforward from equations (16) to (23).

IV. $\mathcal{L}_1$ Adaptive Control of Systems with Disturbances of Unknown Bounds

In this section, based on [28], [29], the $\mathcal{L}_1$ adaptive control approach that borrows insights from sliding mode control to design the adaptive laws is recalled. The main advantage is that the estimation of both the disturbances and their bounds is achieved by using a sliding surface. As a consequence, the performance and the robustness of the control system are improved without assuming prior information about external perturbations.

Given a class of single-input single-output systems defined by

$$\begin{aligned} \dot{x}(t) &= A_m x(t) + b\big(\omega u(t) + \theta^\top x(t) + \eta_m(t)\big) + \eta_u(t,x), \\ y(t) &= c^\top x(t), \end{aligned} \tag{15}$$

where $A_m \in \mathbb{R}^{n\times n}$ is a known Hurwitz matrix that defines the desired dynamics of the system; b, $c \in \mathbb{R}^n$ are known constant vectors; $x(t) \in \mathbb{R}^n$ is the state vector which is assumed available through measurement; $u(t) \in \mathbb{R}$ is the control input; $y(t) \in \mathbb{R}$ is the system output; $\omega \in \mathbb{R}$ is an unknown constant with known sign representing the model input uncertainties; $\theta \in \mathbb{R}^n$ is a vector of constant unknown parameters representing model uncertainties; $\eta_m(t) \in \mathbb{R}$ is an unknown matched disturbance; and $\eta_u(t,x) \in \mathbb{R}^n$ is an unknown unmatched disturbance.

The defined class is equivalent to the systems in (12).

Assumption 2. The non-linear functions $\eta_m(t)$ and $\eta_u(t,x)$ are uniformly bounded, i.e., there exist unknown real constants $L_m > 0$ and $L_u > 0$, such that for all $t \geq 0$ the following bounds hold:

$$|\eta_m(t)| \leq L_m \text{ and } \|\eta_u(t,x)\| \leq L_u.$$

Assumption 3. The unknown model parameters are bounded, i.e., $\theta \in \Theta$, where Θ is a known compact convex set and $0 < \omega_l \leq \omega \leq \omega_u$.

Remark 6. These two assumptions are conventionally acceptable for real systems, given that a superior bound of disturbances and unknown parameters, which the system may hold without being broken, is usually known from technical specifications or engineering insights.

The objective is to design a state-feedback controller to ensure that the output of the system, $y(t)$, tracks a given continuous bounded reference signal $r(t)$.

As shown in Fig. 3, the $\mathcal{L}_1$ adaptive controller consists of three components: the state predictor, the adaptive law with fast adaptation, and the control law with a low-pass filter.

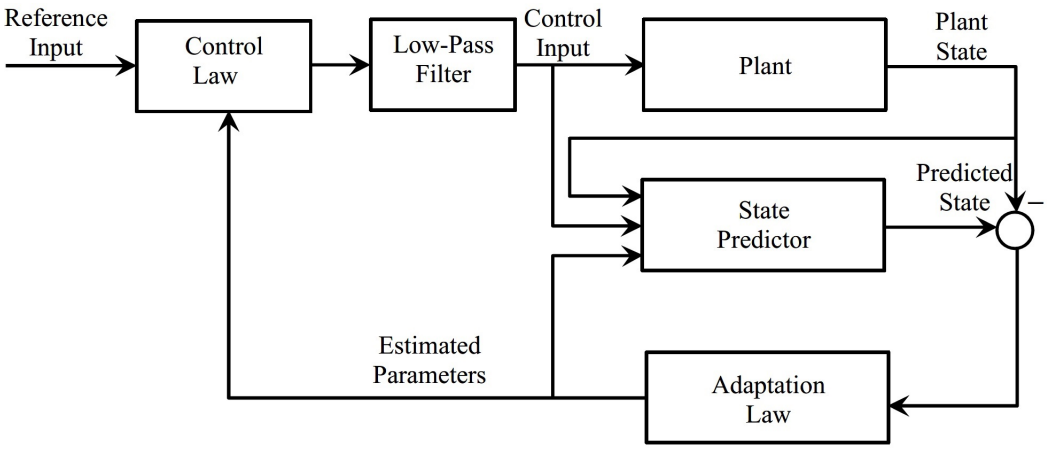

Fig. 3: The $\mathcal{L}_1$ adaptive controller.

The state predictor is defined as

$$\begin{aligned} \dot{\hat{x}}(t) &= A_m\hat{x}(t) + b\big(\hat{\omega}(t)u(t) + \hat{\theta}^\top(t)x(t) + \hat{\eta}_m(t)\big) + \hat{\eta}_u(t), \\ \hat{x}(0) &= x_0, \end{aligned} \tag{16}$$

where $\hat{x}(t)$ is the predicted state and, $\hat{\theta}(t)$, $\hat{\omega}(t)$, $\hat{\eta}_m(t)$, and $\hat{\eta}_u(t)$ are the estimates of the unknown system parameters and external disturbances.

The sliding surface is defined as

$$\sigma(t) = \lambda\tilde{x}(t), \tag{17}$$

where $\tilde{x}(t) = \hat{x}(t) - x(t)$ is the state estimation error and $\lambda \in \mathbb{R}^{1\times n}$ is a constant row vector, chosen such that $\lambda b \neq 0$ and the coefficients $\lambda_i : \ i = 1..n$ form a stable manifold.

The estimation of the matched disturbance $\eta_m(t)$ is defined by

$$\hat{\eta}_m(t) \begin{cases} = -(\lambda b)^{-1}\big(\lambda A_m\tilde{x}(t) + \rho\sigma(t)\big) - \hat{L}_m(t)\frac{\lambda b\sigma(t)}{|\lambda b\sigma(t)|}, & \text{if } \sigma(t) \neq 0, \\ = 0 & \text{otherwise}, \end{cases} \tag{18}$$

where $\rho > 0$ is arbitrary, and the estimated bound $\hat{L}_m(t)$ is given by

$$\dot{\hat{L}}_m(t) = \Gamma|\lambda b\sigma(t)|,\ L_{m0} = \hat{L}_m(0), \tag{19}$$

where $\Gamma \in \mathbb{R}^+$ is the adaptation rate.

The estimation of the unmatched disturbance $\eta_u(t,x)$ is defined by

$$\hat{\eta}_u(t) = \begin{cases} -\hat{L}_u(t)\frac{\big(\lambda\sigma(t)\big)^\top}{\|\lambda\sigma(t)\|}, & \text{if } \sigma(t) \neq 0, \\ 0 & \text{otherwise}, \end{cases} \tag{20}$$

where the estimated bound $\hat{L}_u(t)$ is computed by

$$\dot{\hat{L}}_u(t) = \Gamma\|\lambda\sigma(t)\|,\ L_{u0} = \hat{L}_u(0). \tag{21}$$

The unknown parameters ω and θ are estimated by

$$\begin{aligned} \dot{\hat{\omega}}(t) &= -\Gamma\ \mathrm{Proj}(\hat{\omega}(\mathrm{t}), \lambda \mathrm{b}\sigma(\mathrm{t})\mathrm{u}(\mathrm{t})), \\ \dot{\hat{\theta}}(t) &= -\Gamma\ \mathrm{Proj}(\hat{\theta}(\mathrm{t}), \lambda \mathrm{b}\sigma(\mathrm{t})\mathrm{x}(\mathrm{t})), \end{aligned} \tag{22}$$

where the projection-type adaptive law permits to maintain the unknown parameters within their predefined sets [38].

The control law is given by

$$u(s) = kD(s)\Big(K_g\ r(s) - \hat{\nu}(s) - \phi(s)\hat{\eta}_u(s)\Big), \tag{23}$$

where $k > 0$ is arbitrary, $D(s)$ is a transfer function that leads to a strictly proper stable filter $C(s) = \omega kD(s)/(1+\omega kD(s))$ with $C(0) = 1$; the static gain is chosen as $K_g = -1/(c^\top A_m^{-1} b)$; $\hat{\nu}(s)$ is the Laplace transform of $\hat{\nu}(t) = \hat{\theta}^\top(t)x(t) + \hat{\omega}(t)u(t) + \hat{\eta}_m(t)$; $\phi(s) = c^\top(sI - A_m)^{-1}H_m^{-1}(s)$; $H_m(s) = c^\top(s\mathbb{I} - A_m)^{-1}b$; and $\hat{\eta}_u(s)$ is the Laplace transform of $\hat{\eta}_u(t)$.

Let

$$\begin{aligned} L &= \max_{\theta\in\Theta}\|\theta\|_1, \\ H(s) &= (s\mathbb{I} - A_m)^{-1}b,\ G(s) = H(s)\big(1 - C(s)\big). \end{aligned} \tag{24}$$

The $\mathcal{L}_1$ adaptive controller defined via equations (16) to (23) is subject to the $\mathcal{L}_1$ norm condition:

$$\|G(s)\|_{\mathcal{L}_1} L < 1, \tag{25}$$

where $\|\cdot\|_{\mathcal{L}_1}$ denotes for the $\mathcal{L}_1$ norm.

Moreover, the design of $C(s)$ needs to ensure that

$$G_u(s) = (s\mathbb{I} - A_m)^{-1} - C(s)H(s)\phi(s), \tag{26}$$

is proper and stable.

Controller analysis is detailed in [28], [29], and is omitted here.

Implementation Issues

In practical applications, the sliding surface $\sigma(t)$ does not go to zero due to sampled computation, noisy measurements or other uncertainties. This results in a persistent increase of the estimated bounds of (19) and (21). A solution to this problem is the dead-zone modification. Hence, equations (19) and (21) are modified to be:

$$\dot{\hat{L}}_m(t) = \begin{cases} \Gamma|\lambda b\sigma(t)| & \text{if } |\sigma(t)| > \epsilon_m, \\ 0 & \text{if not,} \end{cases} \tag{27}$$

and

$$\dot{\hat{L}}_m(t) = \begin{cases} \Gamma\|\lambda\sigma(t)\| & \text{if } |\sigma(t)| > \epsilon_u, \\ 0 & \text{if not} \end{cases} \tag{28}$$

where $\epsilon_m \in \mathbb{R}^+$ and $\epsilon_u \in \mathbb{R}^+$ are real constants.

Furthermore, in order to eliminate the chattering, the discontinuous components in equations (18) and (20) are replaced by a smooth sliding mode component to yield

$$\hat{\eta}_m(t) = -(\lambda b)^{-1}\big(\lambda A_m\tilde{x}(t) + \rho\sigma(t)\big) - \hat{L}_m(t)\frac{\lambda b\sigma(t)}{|\lambda b\sigma(t)| + \epsilon}, \tag{29}$$

$$\hat{\eta}_u(t) = -\hat{L}_u(t)\frac{\big(\lambda\sigma(t)\big)^\top}{\|\lambda\sigma(t)\| + \epsilon}, \tag{30}$$

where $\epsilon > 0$ is an arbitrarily small constant. This formulation creates a boundary layer about the switching surface in which the system trajectory will remain. Therefore, the chattering problem can be reduced significantly [39].

V. Simulation Results

In this section, the simulation results for the $\mathcal{L}_1$ adaptive and a linear path-following controllers are presented. The performance of the controllers was evaluated in time-varying wind and in a situation where the airspeed of the UAV varies under wind effect.

First, the design of a linear path-following controller is presented. The objective is to provide a comparison baseline for the performance evaluation of the $\mathcal{L}_1$ adaptive path-following controller.

To provide better robustness against disturbances, the integral of the regulated output error, denoted by e_I, is considered for the linear system in (7). The augmented system can be written as follows

$$\begin{bmatrix} \dot{\bar{x}} \\ \dot{e}_I \end{bmatrix} = \begin{bmatrix} A & 0 \\ -c & 0 \end{bmatrix} \begin{bmatrix} \bar{x} \\ e_I \end{bmatrix} + \begin{bmatrix} b \\ 0 \end{bmatrix} \bar{u}, \tag{31}$$

where A is the system dynamics matrix for the nominal airspeed.

The control law of the system is given by

$$\bar{u} = -k_p^\top \bar{x} - k_I e_I, \tag{32}$$

where $k_I \in \mathbb{R}$ is the integral gain and $k_p \in \mathbb{R}^2$ is the proportional feedback vector that is designed to obtain the same desired system dynamics matrix as the $\mathcal{L}_1$ adaptive controller $A_m = A - b\,k_p^\top$.

It was assumed that the desired airspeed of the UAV is $V_a = 20\,\mathrm{m/s}$ and the maximum turn angle is $|\phi| = 60^0$.

The state-feedback vector k_p was computed by the Linear Quadratic Regulator (LQR) method to obtain desired closed-loop system dynamics with a frequency of $0.7\,\mathrm{rad/s}$ and a damping factor of 0.7. The performance of the $\mathcal{L}_1$ adaptive controller was also compared with the disturbance observer based path-following controller proposed in [40]. The controller and the disturbance observer gains were chosen $k_1 = 0.25$, $k_2 = 12.5$, $k_3 = 25$, $l_x = 10$ and $l_y = 10$, to obtain similar dynamics to the Linear Qaudratic Integral (LQI) and the $\mathcal{L}_1$ adaptive controllers.

The transfer function $D(s)$ of the $\mathcal{L}_1$ adaptive controller was chosen $D(s) = \frac{1}{s(s+9.8)}$ and $k = 36$, which leads to a filter $C(s) = \frac{36}{s^2+9.6s+36}$. The $\mathcal{L}_1$ adaptive controller was designed to be robust against model uncertainties within the compact sets $\omega = [0.5,\ 1.5]$ and $\Theta = \{\vartheta = [\vartheta_1, \vartheta_2] \in \mathbb{R}^2 : \vartheta_i \in [-1,\ 1], i = 1, 2\}$. It is straightforward to show that these parameters verify the stability conditions in (25) and (26).

The UAV was commanded to fly a straight-line path, defined by four (4) waypoints, with the cross-track error d required to be zero. The initial position of the UAV was at the origin of the earth frame.

Simulation results have shown that all controllers present a satisfactory performance when there are no wind disturbances. The trajectories of the UAV relative to the desired path, the cross-track error, the heading error and the commanded roll angle are illustrated in Fig. 4. The

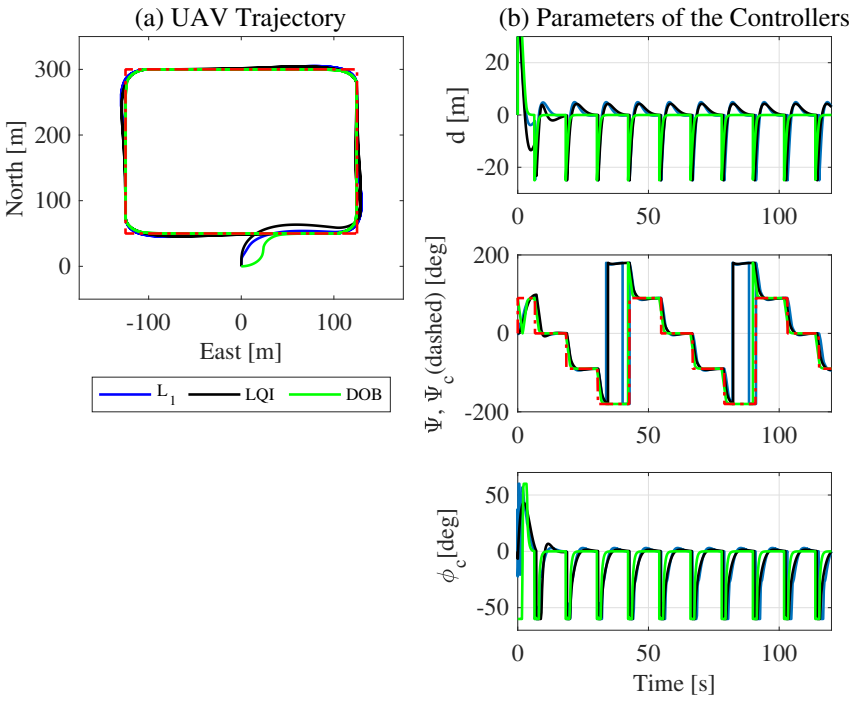

Fig. 4: Simulation results without wind.

presence of peaks in the cross-track error is due to the rolling motion of the UAV when turning at the waypoints. It can be observed that, when the UAV moved from the initial location to the desired path, the $\mathcal{L}_1$ adaptive controller has performed better, although the disturbance observer controller has shown improved performance when turning waypoints, because it does not show the characteristic overshoot of second order systems.

In a second simulation scenario, a time-varying crosswind was introduced. Its velocity was assumed to be a periodic signal, $W_e(t) = 5 + 5\sin(2\pi t)$. Simulation results are shown in Fig. 5. The $\mathcal{L}_1$ adaptive controller performs better than the disturbance observer based controller and the LQI controller in the same wind conditions. In particular, it can be noted that the trajectory of the UAV is smoother and more precise with the $\mathcal{L}_1$ adaptive controller. Moreover, it is clearly illustrated that the cross-track error is not completely eliminated by the LQI and the observed-based controllers. The commanded roll angle of the $\mathcal{L}_1$ adaptive controller is smooth and presents relatively few saturations considering wind conditions. Note that trying to improve the performance of the LQI and the disturbance observer based controllers, by tuning the gains, leads either to instability of the control system or to a worst performance.

The poor performance of the observer based controller is due to the fact that the formulation

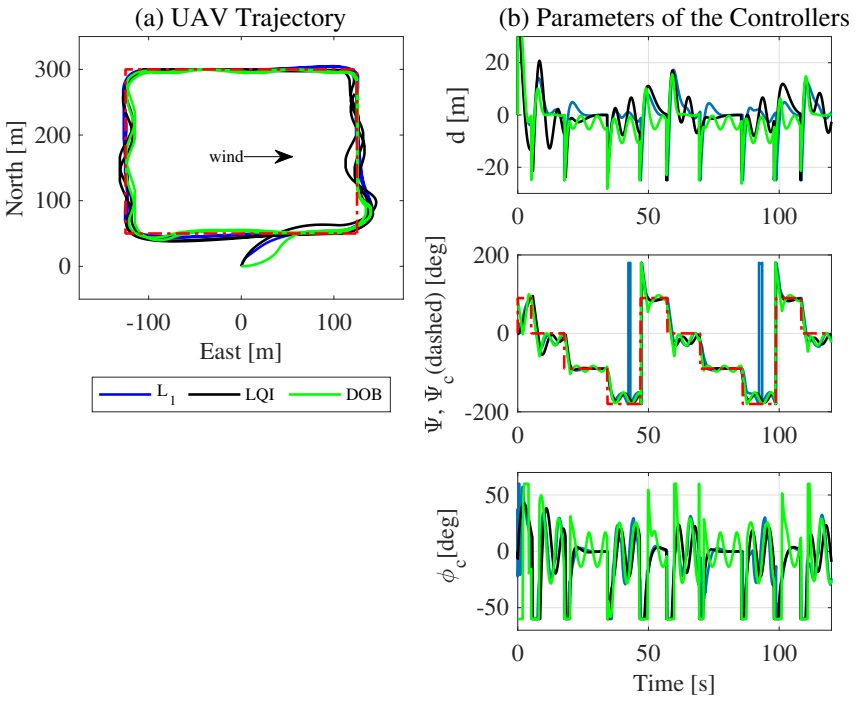

Fig. 5: Simulation results in varying wind.

of the controller in [40] did not not take into account the wind direction relative to the path. This is especially true for the estimation of the trimming angle $\psi_{\hat{0}}$. As a result, it can be noticed that the UAV has produced roll command to counteract wind when it was flying downwind and upwind, which should not be the case. It should be noticed that wind estimator based on [41] has produced good estimation results of the time-varying wind.

Next, as explained above, maintaining a constant airspeed is not feasible in practice, especially in the presence of wind disturbances. In order to simulate this situation, a scenario of a constant wind, with a speed of $10\mathrm{m/s}$, blowing in the easterly direction was introduced. It was furthermore supposed that:

- The airspeed increases by $5\,\mathrm{m/s}$ when the UAV is flying downwind.
- The airspeed decreases by $5\,\mathrm{m/s}$ when the UAV is flying upwind
- The airspeed decreases by $2\,\mathrm{m/s}$ when the UAV is flying crosswind.

This assumption does not have a flight mechanical justification. It is used only for simulation purposes.

It is shown in Fig. 6 that the LQI controller was not able to keep the UAV on the desired path under variations of the airspeed, whereas, as expected, the $\mathcal{L}_1$ adaptive controller has performed

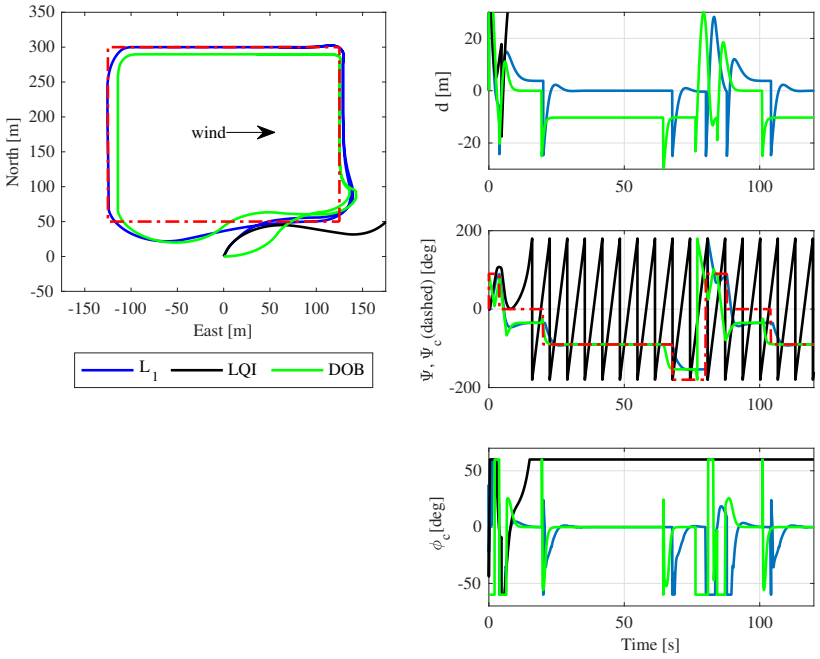

Fig. 6: Simulation results in varying airspeed.

well under the same conditions. To explain this, it can be noted from the model in (8) that unknown time-varying parameters are introduced in the system when the airspeed of the UAV varies due to wind. The robustness of linear controllers is relatively limited in this situation, while the improved performance of the $\mathcal{L}_1$ adaptive controller is due to its ability to compensate unknown parameters and external disturbances. Besides, the observer based controller was able to maintain system stability, however, its performance was poor due to the fact the UAV speed variations has not been considered in controller design.

These simulations conclude that the designed $\mathcal{L}_1$ adaptive path-following system was shown to have better performance than disturbance based and LQI controllers. This is due to its robustness and fast adaptation in the presence of unknown system parameters and external disturbances.

VI. Flight Test Results

In this section, the results in the real flight of the proposed $\mathcal{L}_1$ adaptive path-following controller are presented. Flight experiments were conducted on the Twinstar-II small fixed-wing UAV airframe Fig. 7. The Twinstar-II has a wingspan of $1.4\,\mathrm{m}$ and a weight of about $1.2\,\mathrm{kg}$. It can be monitored and commanded by a PC based ground station which is connected via RF link. The sensor suite of the UAV platform consists of a low cost Inertial Measurement Unit (IMU),

magnetometer, barometric and differential pressure sensors and a GPS receiver. The Twinstar-II was equipped with an on-board computer which consists of a Gumstix Overo SBC and an FPGA [42]. Fig. 8 shows a scheme of the on-board computer system and the applied sensors.

Fig. 7: Twinstar II Small UAV.

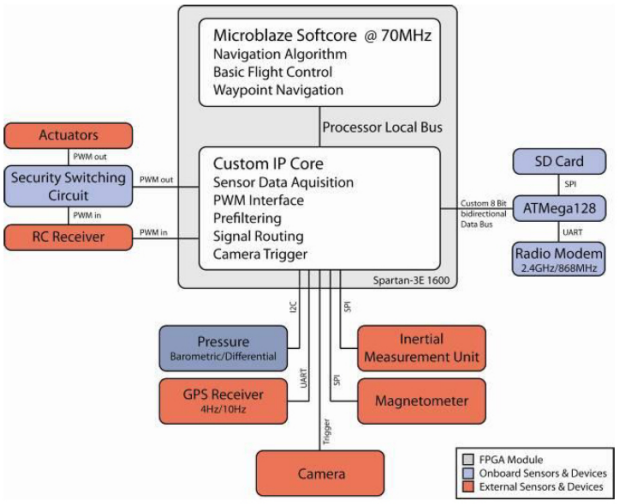

Fig. 8: On-board computer system and applied sensors, actuators and communication interfaces [43].

The autopilot system has a cascaded design, composed of path-following (outer-loop) and attitude (inner-loop) controllers. The $\mathcal{L}_1$ adaptive path-following controller computes the commanded roll angle ϕ_c to achieve desired waypoints. The inner-loop ensures that the states of the UAV track the desired angles using PID based control architecture.

The UAV was commanded to fly a straight-line path, defined by four (4) waypoints, at a constant altitude of $50\,\mathrm{m}$, with the cross-track error d required to be zero. The desired airspeed was set at $V_a = 20\,\mathrm{m/s}$.

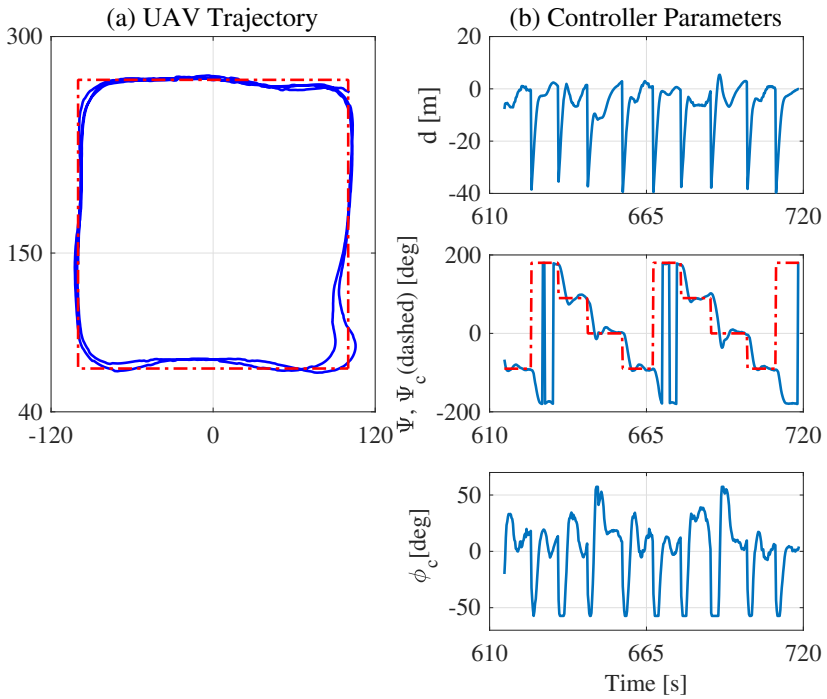

Fig. 9: Flight test of the $\mathcal{L}_1$ adaptive controller without wind.

The preliminary tests were carried out without wind; this permitted further testing in real flight conditions. In Fig. 9 are shown flight test results of the $\mathcal{L}_1$ adaptive controller. Similarly to simulation results, the controller has demonstrated good performance when there are no wind disturbances. It can be seen that the cross-track error converges quickly to zero after turns and the UAV follows the desired path with feasible commands.

The next flight tests were performed in wind which was blowing southerly at approximately $5\,\mathrm{m/s}$, with gusts estimated locally up to $10\,\mathrm{m/s}$. Flight test results for the $\mathcal{L}_1$ adaptive controller in wind are shown in Fig. 10. As it can be seen, the cross-track error is maintained within an acceptable range. Furthermore, it can be observed that the UAV produces the commanded roll angle ϕ_c that compensates wind effect.

VII. Summary

This paper presents an approach for adaptive path-following of small fixed-wing UAVs. The design was made for 2D straight and circular paths. The proposed approach is based on the $\mathcal{L}_1$ adaptive control for disturbances of unknown bounds. The adaptive controller has shown better performance in simulations compared to LQI and disturbance observer based controllers. The

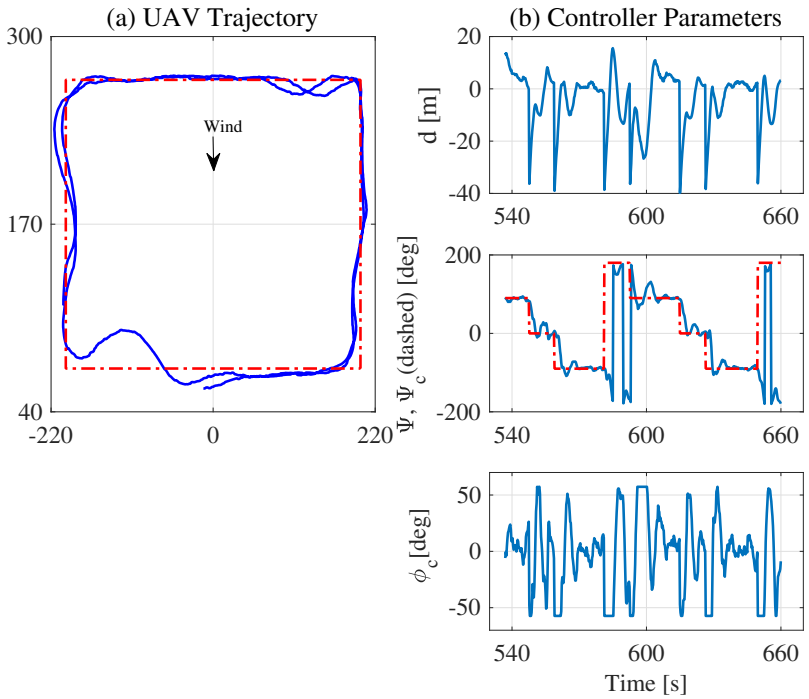

Fig. 10: Flight test of the $\mathcal{L}_1$ adaptive controller in wind.

controller was demonstrated in real flight under winds up to 10 m/s, representing 50% of the airspeed of the UAV. This approach makes clear statements for performance specifications of the controller and relaxes the common constant wind velocity assumption. This makes the design more realistic and the analysis more rigorous, because in practice, the wind velocity may be time varying, such as wind shear or wind gusts.

Even though the framework developed in this paper has been successfully demonstrated in practice, a more realistic approach to the problem of path following under wind disturbance is to consider that in the real world, wind velocity is completely unpredictable, i.e., it is a stochastic phenomenon. Such an approach needs to borrow tools from stochastic analysis. Future research can also investigate the design based on cascaded $\mathcal{L}_1$ adaptive architecture, while the attitude controller is based on $\mathcal{L}_1$ adaptive control. The main theoretical challenge is to analyse stability of the system. Another direction is the integrated guidance and control, that combines both the outer-loop and the inner-loop in the same control loop of the UAV. Moreover, the formulation of UAVs path-following as a problem of control design in the presence of uncertainties and external disturbances opens a gap for the introduction of a large panel of control methodologies for the development of robust path-following in wind.

ACKNOWLEDGEMENTS

I would like to express my gratitude to my PhD supervisor Pr. Walter Fichter, University of Stuttgart, for his guidance and detailed advice through the elaboration of this research. I would also like to express my appreciation to my thesis referee Pr. Florian Holzapfel, University of Munich, for his insights and comments. I also wish to thank my colleague Dr. James Whidborne for his valuable feedback.

REFERENCES

[1] R. Austin, *Unmanned aircraft systems: UAVs design, development and deployment*. John Wiley & Sons, 2011, vol. 54.

[2] P. B. Sujit and S. Saripalli, "Unmanned aerial vehicle path following," *IEEE Control Systems Magazine*, no. February, 2014.

[3] J. H. Blakelock, *Automatic control of aircraft and missiles*. John Wiley & Sons, 1991.

[4] K. Hassan, *Nonlinear systems*. Prentice-Hall, 2002.

[5] D. R. Nelson, D. B. Barber, T. W. McLain, and R. W. Beard, "Vector field path following for miniature air vehicles," *Robotics, IEEE Transactions on*, vol. 23, no. 3, pp. 519–529, 2007.

[6] N. Ceccarelli, J. J. Enright, E. Frazzoli, S. J. Rasmussen, and C. J. Schumacher, "Micro UAV path planning for reconnaissance in wind," in *American Control Conference, 2007. ACC'07*. IEEE, 2007, pp. 5310–5315.

[7] T. G. McGee and J. K. Hedrick, "Path planning and control for multiple point surveillance by an unmanned aircraft in wind," in *American Control Conference, 2006*. IEEE, 2006.

[8] J. Osborne and R. Rysdyk, "Waypoint guidance for small UAVs in wind," *AIAA Infotech Aerospace*, vol. 193, no. 1-4, pp. 1–12, 2005.

[9] R. Rysdyk, "Unmanned aerial vehicle path following for target observation in wind," *Journal of Guidance, Control, and Dynamics*, vol. 29, no. 5, pp. 1092–1100, 2006.

[10] R. W. Beard, J. Ferrin, and J. Humpherys, "Fixed wing UAV path following in wind with input constraints," *IEEE Transactions on Control Systems Technology*, vol. 22, no. 6, pp. 2103–2117, 2014.

[11] A. Brezoescu, R. Lozano, and P. Castillo, "Lyapunov-based trajectory tracking controller for a fixed-wing unmanned aerial vehicle in the presence of wind," *International Journal of Adaptive Control and Signal Processing*, vol. 29, no. 3, pp. 372–384, 2015.

[12] S. Fari, X. Wang, S. Roy, and S. Baldi, "Addressing unmodeled path-following dynamics via adaptive vector field: a UAV test case," *IEEE Transactions on Aerospace and Electronic Systems*, vol. 56, no. 2, pp. 1613–1622, 2019.

[13] C. Liu, O. McAree, and W.-H. Chen, "Path-following control for small fixed-wing unmanned aerial vehicles under wind disturbances," *International Journal of Robust and Nonlinear Control*, vol. 23, no. 15, pp. 1682–1698, 2013.

[14] A. Ratnoo, P. Sujit, and M. Kothari, "Adaptive optimal path following for high wind flights," in *18th IFAC World Congress, Milano, Italy*, vol. 2, 2011.

[15] X. Wang, S. Roy, S. Farì, and S. Baldi, "The problem of reliable design of vector-field path following in the presence of uncertain course dynamics," *IFAC-PapersOnLine*, vol. 53, no. 2, pp. 9399–9404, 2020.

[16] B. Zhou, H. Satyavada, and S. Baldi, "Adaptive path following for unmanned aerial vehicles in time-varying unknown wind environments," in *American Control Conference (ACC), 2017*. IEEE, 2017, pp. 1127–1132.

[17] J. Yang, C. Liu, M. Coombes, Y. Yan, and W.-H. Chen, "Optimal path following for small fixed-wing UAVs under wind disturbances," *IEEE Transactions on Control Systems Technology*, 2020.

[18] N. Hovakimyan and C. Cao, $\mathcal{L}_1$ *adaptive control theory: Guaranteed robustness with fast adaptation*. Siam, 2010, vol. 21.

[19] R. Beard, C. Cao, and N. Hovakimyan, "An $\mathcal{L}_1$ adaptive pitch controller for miniature air vehicles," in *AIAA guidance, navigation, and control conference and exhibit*, 2006, p. 6777.

[20] E. Capello, G. Guglieri, F. Quagliotti, and D. Sartori, "Design and validation of an $\mathcal{L}_1$ adaptive controller for mini-UAV autopilot," *Journal of Intelligent & Robotic Systems*, vol. 69, no. 1-4, pp. 109–118, 2013.

[21] I. Kaminer, A. Pascoal, E. Xargay, N. Hovakimyan, C. Cao, and V. Dobrokhodov, "Path following for small unmanned aerial vehicles using $\mathcal{L}_1$ adaptive augmentation of commercial autopilots," *Journal of guidance, control, and dynamics*, vol. 33, no. 2, pp. 550–564, 2010.

[22] J. Wang, V. Patel, C. A. Woolsey, N. Hovakimyan, and D. Schmale, "$\mathcal{L}_1$ adaptive control of a UAV for aerobiological sampling," in *American Control Conference, 2007. ACC'07*. IEEE, 2007, pp. 4660–4665.

[23] Y. Zhou, H. Liu, H. Guo, and X. Duan, "$\mathcal{L}_1$ adaptive dynamic inversion attitude control for unmanned aerial vehicle with actuator failures," *Proceedings of the Institution of Mechanical Engineers, Part G: Journal of Aerospace Engineering*, vol. 233, no. 11, pp. 4129–4140, 2019.

[24] H. Beikzadeh and G. Liu, "Trajectory tracking of quadrotor flying manipulators using $\mathcal{L}_1$kotaru, adaptive control," *Journal of the Franklin Institute*, vol. 355, no. 14, pp. 6239–6261, 2018.

[25] E. Capello, F. Quagliotti, and R. Tempo, "Randomized approaches for control of quadrotor UAVs," *Journal of Intelligent & Robotic Systems*, vol. 73, no. 1-4, pp. 157–173, 2014.

[26] P. Kotaru, R. Edmonson, and K. Sreenath, "Geometric $\mathcal{L}_1$ adaptive attitude control for a quadrotor unmanned aerial vehicle," *Journal of Dynamic Systems, Measurement, and Control*, vol. 142, no. 3, 2020.

[27] W. Zhou, X. Wang, B. Liu, J. Liu, and Y. Chang, "Design of attitude loop controller for six-rotor UAV based on $\mathcal{L}_1$ adaptive method," in *Journal of Physics: Conference Series*, vol. 1486, no. 7. IOP Publishing, 2020, p. 072065.

[28] T. Souanef, *Adaptive Guidance and Control of Small Unmanned Aerial Vehicles*. Germany: Shaker Verlag, 2019.

[29] T. Souanef, A. Boubakir, and W. Fichter, "L1 adaptive control of systems with disturbances of unknown bounds," in *Advances in Aerospace Guidance, Navigation and Control: Selected Papers of the Third CEAS Specialist Conference on Guidance, Navigation and Control held in Toulouse*. Springer, 2015, p. 151.

[30] I. Kaminer, O. Yakimenko, V. Dobrokhodov, A. Pascoal, N. Hovakimyan, V. Patel, C. Cao, and A. Young, "Coordinated path following for time-critical missions of multiple UAVs via $\mathcal{L}_1$ adaptive output feedback controllers," in *AIAA Guidance, Navigation and Control Conference and Exhibit*, 2007, p. 6409.

[31] P. De Monte and B. Lohmann, "Position trajectory tracking of a quadrotor based on $\mathcal{L}_1$ adaptive control," *at–Automatisierungstechnik*, vol. 62, no. 3, pp. 188–202, 2014.

[32] G. Han, J. Zhou, J. Guo, and Q. Lu, "A longitudinal trajectory tracking method with $\mathcal{L}_1$ adaptive control for hypersonic reentry vehicles," *Transactions of the Institute of Measurement and Control*, vol. 42, no. 3, pp. 386–403, 2020.

[33] H. Xu, P. Oliveira, and C. G. Soares, "$\mathcal{L}_1$ adaptive backstepping control for path-following of underactuated marine surface ships," *European Journal of Control*, vol. 58, pp. 357–372, 2021.

[34] Z. Zuo and S. Mallikarjunan, "$\mathcal{L}_1$ adaptive backstepping for robust trajectory tracking of UAVs," *IEEE Transactions on Industrial Electronics*, vol. 64, no. 4, pp. 2944–2954, 2016.

[35] R. Mahony, V. Kumar, and P. Corke, "Multirotor aerial vehicles: Modeling, estimation, and control of quadrotor," *IEEE Robotics and Automation magazine*, vol. 19, no. 3, pp. 20–32, 2012.

[36] E. Lavretsky and K. A. Wise, "Robust adaptive control," in *Robust and Adaptive Control*. Springer, 2013, pp. 317–353.

[37] V. G. Rao and D. S. Bernstein, "Naive control of the double integrator," *IEEE Control Systems Magazine*, vol. 21, no. 5, pp. 86–97, 2001.

[38] J.-B. Pomet and L. Praly, "Adaptive nonlinear regulation: estimation from the lyapunov equation," *Automatic Control, IEEE Transactions on*, vol. 37, no. 6, pp. 729–740, 1992.

[39] G. Ambrosino, G. Celektano, and F. Garofalo, "Variable structure model reference adaptive control systems," *International Journal of Control*, vol. 39, no. 6, pp. 1339–1349, 1984.

[40] C. Liu, O. McAree, and W.-H. Chen, "Path following for small UAVs in the presence of wind disturbance," in *Proceedings of 2012 UKACC International Conference on Control*. IEEE, 2012, pp. 613–618.

[41] W.-H. Chen, "Disturbance observer based control for nonlinear systems," *IEEE/ASME transactions on mechatronics*, vol. 9, no. 4, pp. 706–710, 2004.

[42] F. Weimer, M. Trittler, A. Joos, M. Gros, A. Posch, and W. Fichter, "FPGA-based onboard computer system for mini aerial vehicles," in *International Micro Air Vehicle Conference, Braunschweig*, 2010.

[43] N. Haala, M. Cramer, F. Weimer, and M. Trittler, "Performance test on UAV-based photogrammetric data collection," *International Archives of the Photogrammetry, Remote Sensing and Spatial Information Sciences*, vol. 38, no. 6, 2011.